

Master 1 Internship: The impact of Arctic sea ice variability on the Northern latitude hydrological cycle in models and reanalyses.



Jökulsárlón, South Iceland

Credit: © trebro / Fotolia

Mickaël LALANDE

Tuteur: Olga ZOLINA (avec Maria SANTOLARIA-OTIN et Ambroise DUFOUR)

Master 1 Sciences de la Terre et des planètes, Environnement

Parcours Atmosphère, Climat et Surfaces continentales

30/04/2018 - 27/07/2018 (3 mois)



Master Sciences de la Terre et de l'Environnement

Attestation de non plagiat

Je soussigné (Prénom NOM) :

Mickaël LALANDE

Auteur du mémoire :

The impact of Arctic sea ice variability on the Northern latitude hydrological cycle in models and reanalyses.

Déclare sur l'honneur que ce mémoire est le fruit d'un travail personnel et que je n'ai ni contrefait, ni falsifié, ni copié tout ou partie de l'oeuvre d'autrui afin de la faire passer pour la mienne.

Toutes les sources d'information utilisées et les citations d'auteur ont été mentionnées conformément aux usages en vigueur.

Je suis conscient que le fait de ne pas citer une source ou de ne pas la citer clairement et complètement est constitutif de plagiat, et que le plagiat est considéré comme une faute grave au sein de l'Université, pouvant être sévèrement sanctionnée par la loi.

Fait à Saint-Martin-d'Hères,

Le 27 juillet 2018

Signature de l'étudiant

A handwritten signature in black ink, appearing to be 'M. Lalande', written over a horizontal line.

Abstract

We used two atmospheric models: the Community Atmosphere Model version 4 (CAM4) and the Whole Atmospheric Community Climate Model (WACCM), and two experiments (*Ogawa et al.*, 2018) for the period 1982-2014. These two experiments were designed to show the impact of sea ice changes on climate variability independently of sea surface temperature (SST), and 20 ensemble members were produced to analyze the internal variability of the climate system. Our goal is to investigate the possible impact of sea ice changes on Arctic climate variability. We used 2m temperature, vertically integrated water vapor content, net precipitation and snow cover. The first part of our study has been focused on the circumpolar Arctic domain (north of 50°N). In the second part, we considered the warm Arctic-cold Siberian (WACS) pattern. In the last part, we looked at the moisture budget of the polar cap for the Arctic domain. We considered two seasons: the so-called Arctic winter (JFMA) and Arctic summer (JASO). During winter, sea ice almost does not have any impact on the mid to high latitude climate. During the Arctic summer, the variation of sea ice likely contributes to almost half of the trends observed over all the Arctic domain. Changes in sea ice do not show a significant impact on the Siberian cooling. Study of each ensemble member shows that the WACS pattern is likely associated with internal atmospheric variability. Finally, we found a significant overestimation of the net precipitation in the Arctic region in the models comparing to ERA-Interim reanalysis.

Résumé

Nous avons utilisé deux modèles atmosphériques: le Community Atmosphere Model version 4 (CAM4) et le Whole Atmospheric Community Climate Model (WACCM) et deux expériences (*Ogawa et al.*, 2018) pour la période 1982-2014. Ces deux expériences ont été conçues pour montrer l'impact des changements de la glace de mer sur la variabilité climatique indépendamment de la température de surface de la mer et 20 membres ont été produits afin d'analyser la variabilité interne du système climatique. Notre objectif est d'étudier l'impact possible des changements de la glace de mer sur la variabilité du climat en Arctique. Nous avons utilisé la température de surface, la vapeur d'eau intégrée verticalement, la précipitation nette et la couverture de neige. La première partie de notre étude a porté sur le domaine Arctique circumpolaire (au nord de 50 °N). Dans la deuxième partie, nous avons étudié le phénomène Arctique chaud-Sibérie froide (WACS). Dans la dernière partie, nous avons évalué le bilan d'humidité du cercle polaire Arctique. Nous avons considéré deux saisons: l'hiver arctique (JFMA) et l'été arctique (JASO). En hiver, les variations de la glace de mer n'ont pratiquement aucun impact sur le climat des hautes-moyennes latitudes. En revanche, pendant l'été arctique, ces variations contribuent notablement aux tendances observées. Pour le refroidissement sibérien, les variations de la glace de mer ne semblent pas en cause. L'étude de chaque membre montre que le phénomène WACS est probablement associé à la variabilité interne de l'atmosphère. Enfin, nous avons constaté une surestimation importante de la précipitation nette dans la région Arctique pour les modèles par rapport à la réanalyse ERA-Interim.

Contents

1	Introduction	3
2	Data and methods	4
2.1	Models and experiments	4
2.2	Reanalyses	5
2.3	Variables	6
2.3.1	2m temperature	6
2.3.2	Vertically integrated water vapor (IWV)	6
2.3.3	Net precipitation (P-E)	7
2.3.4	Land snow cover	7
2.4	Moisture budget of the atmosphere	8
2.5	Domains and periods	8
2.6	Numerical methods	9
3	Results	9
3.1	Arctic domain	10
3.1.1	Climatology	10
3.1.2	Annual cycle	11
3.1.3	Trends	12
3.2	Siberian cooling	14
3.2.1	Reanalysis and models comparison	14
3.2.2	Internal variability	15
3.3	Polar cap moisture budget	16
4	Discussion	17
5	Conclusion	18
A	IWV uncertainty estimation	21
B	Net precipitation	22
C	Reanalyses and model comparison for trends	23

1 Introduction

From the last decades, the Arctic region has warmed more than twice as fast as the Northern Hemisphere (NH) with the most significant differences in winter (Figure 1). This phenomenon is known as Arctic amplification (*Serreze and Barry, 2011; Cohen et al., 2014*).

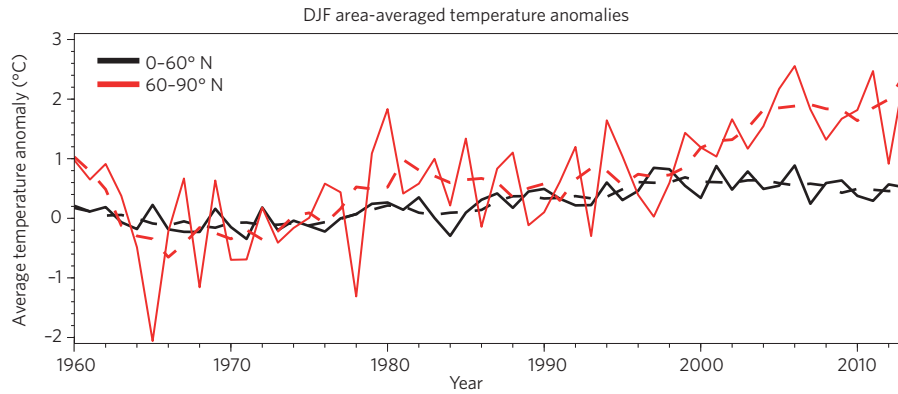


Figure 1: Adapted from *Cohen et al. (2014)* - Winter (DJF) area-averaged surface temperature anomalies ($^{\circ}\text{C}$) from 0° to 60°N (solid black line) and 60° to 90°N (solid red line) along with five-year smoothing (dashed black and red lines, respectively). Data from the National Aeronautics and Space Administration Goddard Institute for Space Studies temperature analysis (<http://data.giss.nasa.gov/gistemp>).

Meanwhile, since 1979, a decline of Arctic sea ice extent is observed all months of the year (see <http://www.meereisportal.de/en/seaicetrends/monthly-mean-arctic/>) with a maximum retreat in September and a decreasing trend of -12.4% per decade from 1979 to 2010 (*Stroeve et al., 2012*) (Figure 2).

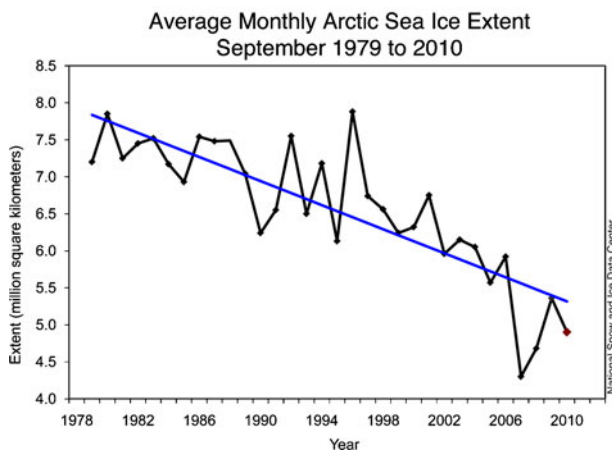


Figure 2: Adapted from *Stroeve et al. (2012)* - Time-series of monthly averaged September sea ice extent with linear trend line.

These changes in the Arctic system have been observed in conjunction with more frequent extreme weather events across the NH mid-latitudes and with a winter cooling of the mid-latitudes in recent years, especially strong over Siberia (*Cohen et al., 2014*) (Figure 3). This phenomenon, known as “warm Arctic-cold Siberia”

(WACS), has already occurred in the early twentieth-century from around 1910 to 1940 (*Wegmann et al.*, 2018); however, the exact mechanism behind this dipolar temperature pattern is still under debate.

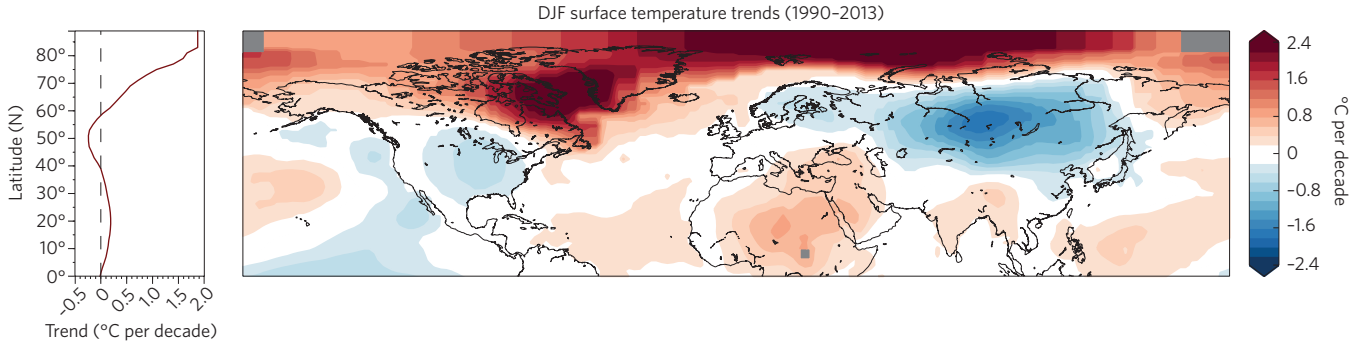


Figure 3: Adapted from *Cohen et al.* (2014) - Linear trend ($^{\circ}\text{C}$ per 10 years) in December-February (DJF) mean surface air temperatures from 1990-1991 to 2013-2014. Shading interval 0.2°C per 10 years. Dark grey indicates points with insufficient samples to calculate a trend. Data from the National Aeronautics and Space Administration Goddard Institute for Space Studies temperature analysis (<http://data.giss.nasa.gov/gistemp>).

This study aims to look at the possible influence of the recent Arctic sea ice variability on the 2m temperature and the major hydrological cycle variables such as water vapor, net precipitation and snow cover. The monthly average output of a model simulation performed by *Ogawa et al.* (2018) is used to better address the relative contributions of Arctic sea ice, sea surface temperature (SST), and internal atmospheric dynamics. Section 2 describes the data and methods, then the results are presented in section 3 before discussing them in section 4. Finally section 5 summarize all this study.

2 Data and methods

2.1 Models and experiments

We used two atmospheric climate models: the Community Atmosphere Model version 4 (CAM4) (*Neale et al.*, 2013) and the Whole Atmospheric Community Climate Model (WACCM) (*Marsh et al.*, 2013). Their resolution is given in Table 1. Both of them are part of the Community Climate System Model (CCSM) (<http://www.cesm.ucar.edu/models/ccsm4.0/>) that is a coupled climate model for simulating the Earth’s climate system. WACCM is a “high top” superset of CAM4, it is extended in altitude to the lower thermosphere so that stratospheric events can be better simulated (e.g., sudden stratospheric warmings, development of the ozone hole).

Model	Horizontal resolution	Vertical resolution
CAM4	0.9° latitude by 1.25° longitude	26 vertical levels up to 3 hPa
WACCM	0.9° latitude by 1.25° longitude	66 vertical levels up to 5.1×10^{-6} hPa

Table 1: Horizontal and vertical resolutions of the models CAM4 and WACCM.

Experiment	Sea ice forcing	SST forcing
SST-SIC-EXP	Daily varying sea ice	Daily varying SST
SIC-EXP	Daily varying sea ice	Daily SST climatology

Table 2: Experiment forcing description.

To see the impacts of Arctic sea ice and SST on the Northern latitude climate, *Ogawa et al.* (2018) performed two different experiments with 5 different atmospheric models (2 of them are described above and were used in this study) for the period from 1982 to 2014. Both experiments were forced by prescribed SST and sea ice from the National Oceanic and Atmospheric Administration (NOAA) Optimum Interpolation 1/4 Degree Daily Sea Surface Temperature Analysis version2, AVHRR-only product (Reynolds et al., 2007) (provided from <http://www.ncdc.noaa.gov/sst/index.php>) as described in Table 2. The first experiment (SST-SIC-EXP) is the most realistic, using daily varying observations for both SST and sea ice, while the second experiment (SIC-EXP) is designed to exhibit the impact of sea ice only. Indeed, the daily climatology (daily mean value over the 1982-2014 period) imposes a realistic SST annual cycle but without interannual variability, while the sea ice varies as in the first experiment.

The experiments were repeated using slightly different initial conditions to make 20 ensemble members for each model to take into account the chaotic nature of atmospheric dynamics¹. Indeed, the atmosphere is a chaotic system, so slightly different initial conditions can lead to significantly different outcomes. Changing the initial conditions is a common technic in atmospheric modeling to represent these stochastic effects. Each member represents a possible scenario. Then, the average of these members, called *ensemble mean*, yields an average scenario that reduces the impact of the internal variability of the atmosphere.

2.2 Reanalyses

A meteorological reanalysis is a combination between historical observations and modeling. Their goal is to give a past state of the atmosphere by interpolating in time and space the observations using dynamical and physical models. The very important advantage of using reanalyses in comparison with observations

¹For more detail on data and experiments please refer to *Ogawa et al.* (2018).

is that reanalyses provide gridded global variables over the atmosphere. However, reanalyses are model data, so they need to be used with caution in some situations, in particular for computing trends when significant changes happened in the observational system, e.g., the start of satellite observations in 1979 or the growing network of observations (*Bengtsson et al.*, 2004).

We used monthly values of the 2-meter temperature, total precipitation, evaporation and vertical integral of water vapor from the ERA-Interim reanalysis (*Dee and Coauthors*, 2011) that covers the period 1979 to present. This reanalysis is provided by the European Centre for Medium-Range Weather Forecasts (ECMWF) with a spatial resolution of approximately 80 km (T255 spectral) on 60 vertical levels from the surface up to 0.1 hPa. For the snow cover², we used monthly values from NOAA-CIRES 20th Century Reanalysis (V2c) provided by the NOAA/OAR/ESRL PSD, Boulder, Colorado, USA, from their Web site at <https://www.esrl.noaa.gov/psd/> which covers the period from 1851 to 2014. The model has a spatial resolution of nearly 200-km on an irregular Gaussian grid in the horizontal (corresponding to a spherical harmonic representation of model fields truncated at total wavenumber 62, T62) and 28 vertical levels using a finite differencing.

2.3 Variables

We used monthly average data outputs from the models and experiments described before. To see the impact of sea ice on Arctic climate we considered 4 variables linked to the hydrological cycle: 2m temperature, vertically integrated water vapor (IWV), net precipitation which is precipitation minus evaporation (P-E) and snow cover.

2.3.1 2m temperature

The 2-meter temperature is the reference height temperature that is given for 2-meter height from the surface (observational height). Temperature is closely related to other variables in the hydrological cycle through the Clausius-Clapeyron relation. It drives, for example, the changes of phase: condensation, melting and evaporation.

2.3.2 Vertically integrated water vapor (IWV)

IWV was not provided as a model output, so that we performed vertical integration of specific humidity q (mass of water vapor per unit mass of moist air). For both models q was given on 19 pressure levels

²Not available in ERA-Interim.

from $p_0 = 1000$ hPa to $p_N = 5$ hPa (above this level, moisture concentration become negligible). The first levels were already masked when the surface pressure is lower than p_0 (e.g., orographic effect, depression system). As suggested by *Dufour* (2016), we used a trapezoidal integration method by interpolating the first level to the surface with the first value of specific humidity³:

$$\int_0^{p_S} q \frac{dp}{g} \simeq q(p_{n_0}) \times \frac{p_S - p_{n_0}}{g} + \sum_{n=n_0}^{N-1} \frac{1}{2} \times [q(p_{n+1}) + q(p_n)] \times \frac{p_n - p_{n+1}}{g} \quad (1)$$

where q is the specific humidity, p the pressure, g the gravity acceleration and N the number of pressure levels. The subscript S correspond to the surface and n_0 to the first level not masked.

2.3.3 Net precipitation (P-E)

The net precipitation (precipitation minus evaporation or P-E) is an important variable for the moisture budget of the atmosphere: it is the moisture that comes from elsewhere rather than being recycled. The evaporation was also not directly provided as a model output, however the latent heat flux LE ($W/m^2 = J/(m^2.s)$) was available. Thus, it is only a matter of unit conversion using the specific latent heat L (J/kg) depending on the changing phase and the density of water (knowing that $1 kg/m^3$ of water correspond to $1 mm$ in hydrology). The empirical formulas from *Rogers and Yau* (1989) were used to compute the specific latent heat: $L_{water}(T) \simeq 2500.8 - 2.36 \times T + 0.0016 \times T^2 - 0.00006 \times T^3$ in J/g (temperatures from -25 °C to 40 °C) and $L_{ice}(T) \simeq 2834.1 - 0.29 \times T + 0.004 \times T^2$ in J/g (temperatures from -40 °C to 0 °C) where the temperature T is the skin (or ground) temperature in Celsius degrees.

Therefore, for evaporation (lands and water area), we applied: $E_{water} \simeq LE/L_{water}(T)$ and for sublimation (snow and ice area) $E_{ice} \simeq LE/L_{ice}(T)$. For the grid cells where a mix of ice and water change phase take place, we computed E with the corresponding weight. For example if a cell has 30% of snow, we computed: $E_{tot} = 0.3 \times E_{ice} + 0.7 \times E_{water}$. This computation provides a monthly average evaporation rate (mm/s) that fits with the precipitation that is expressed in the same units.

2.3.4 Land snow cover

Snow cover plays an important role in the climatic system by changing significantly the albedo of the surface. Snow is essentially located in the NH areas and is suspected to be involved in polar amplification (*Brutel-Vuilmet et al.*, 2013). The monthly average snow cover is provided as a percentage for each grid

³Actually, the monthly average values introduced an additional numerical uncertainty because the first level not masked was sometimes 2 levels higher than the mean surface pressure (see Appendix A for more details).

cell. We chose to keep only the land snow cover (where the albedo impact is more important), therefore we applied a mask using the CCSM4 fixed historical land area fraction up to 50% and the fixed historical fraction of grid cell covered with glacier lower than 15% (available on <https://esgf-node.llnl.gov/search/cmip5/>)⁴. The thresholds were chosen before this study with the aim to find a compromise between keeping the maximum of snow cover with as less permanent ice as possible (see Figure 4).

2.4 Moisture budget of the atmosphere

The moisture budget of an atmospheric column can be analyzed by evaluating either side of the moisture balance equation:

$$\frac{\partial}{\partial t} \int_0^{p_S} q \frac{dp}{g} + (P - E) = -\text{div} \int_0^{p_S} q \mathbf{V} \frac{dp}{g} \quad (2)$$

where q is specific humidity, g the standard gravity, p the pressure vertical coordinate, \mathbf{V} the wind, E evaporation, P precipitation, and p_S the surface pressure. The first term on the left-hand side, the precipitable water tendency, is typically negligible compared to the other terms for yearly time scales (*Peixoto et al.*, 1992).

Equation (2) shows that the variation of water vapor in the atmosphere plus the net precipitation should be equal to the moisture convergence. However, the monthly average data does not allow to compute this right-hand side term, because the product of the mean specific humidity \bar{q} and mean wind $\bar{\mathbf{V}}$ is not equal to the mean of both because of fluctuations: $\overline{q\mathbf{V}} = \bar{q} \bar{\mathbf{V}} + \overline{q'\mathbf{V}'}$, and this last term of fluctuations can have a significant contribution on a monthly timescale (*Dufour*, 2016). Since we have only monthly data, the moisture budget was estimated via the net precipitation.

2.5 Domains and periods

We used three domains in this study (Figure 4) and two different time periods (the second time period was defined in order to fit the WACS pattern better):

Arctic domain (1982-2014) defined up to 50°N that is mainly used for comparing models and experiments for all variables and see the potential impact of sea ice at the mid and high latitude climate.

For this domain, we used the ice-free land mask described in the previous section.

⁴The historical experiment from the Coupled Model Intercomparison Project Phase 5 (CMIP5) is set from 1850 to 2005, so it is maybe not the most realistic way to get a constant area for glacier during our study period (1982-2014), but this allows to keep the same surface.

Siberian region (1990-2013) was used for investigating the specific cold pattern that can be seen above East-Eurasia (Figure 3). I defined the region by 70°E - 130°E 40°N - 65°N and the period to fit the most significant 2m temperature negative trends (see Section 3.2).

Polar cap (1982-2014) defined north of 70°N was used for computing the moisture budget and comparing it to another team project.

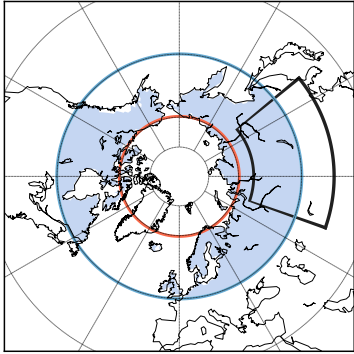


Figure 4: Studied domains: inside the blue circle is the Arctic domain ($>50^{\circ}\text{N}$) including in light blue shading the ice-free land area (land $>50\%$ and permanent ice $<15\%$); inside the red circle is the polar cap ($>70^{\circ}\text{N}$); the black box represents the Siberian region (70°E - 130°E 40°N - 65°N).

2.6 Numerical methods

Data were provided as NetCDF files. I used Python 2.7 for reading, computing and plotting data. In particular for manipulating the data, I used the library *xarray* and for plotting the library *Basemap*. The projections used in this report are mainly the North Pole Stereographic projection and punctually also the Equidistant Cylindrical Projection. All data (when needed) were regridded using the Climate Data Operators version 1.7.2 (CDO) with the bilinear method. For linear regression, the function *linregress* was used from the library *Scipy* that also return a p-value based on a Wald Test with t-distribution (null hypothesis being the slope is zero).

3 Results

We present the results in three different sections: a first section investigates the differences in the Arctic domain between the models and experiments to see the impact of the variation of sea ice on all variables. Then, each of the last two sections investigates a particular phenomenon to answer the following questions: are these models and experiments able to reproduce the recent Siberian cooling pattern and are they able to simulate well the moisture budget for the polar cap?

3.1 Arctic domain

For clarity and because of similarities between seasons, the results are presented for the Arctic seasons: winter (January to April or JFMA) and summer (July to October or JASO) as suggested by *Tilinina et al.* (2014). To focus on the impact of sea ice, we study the ensemble mean (average of the 20 members) to reduce the internal variability of the atmosphere.

3.1.1 Climatology

The climatology represents a mean state of the atmosphere over a considered period. Figure 5 shows the ensemble mean climatology for the model CAM4 and experiment SST-SIC-EXP (the other model and experiments are not shown because of similar spatial distribution).

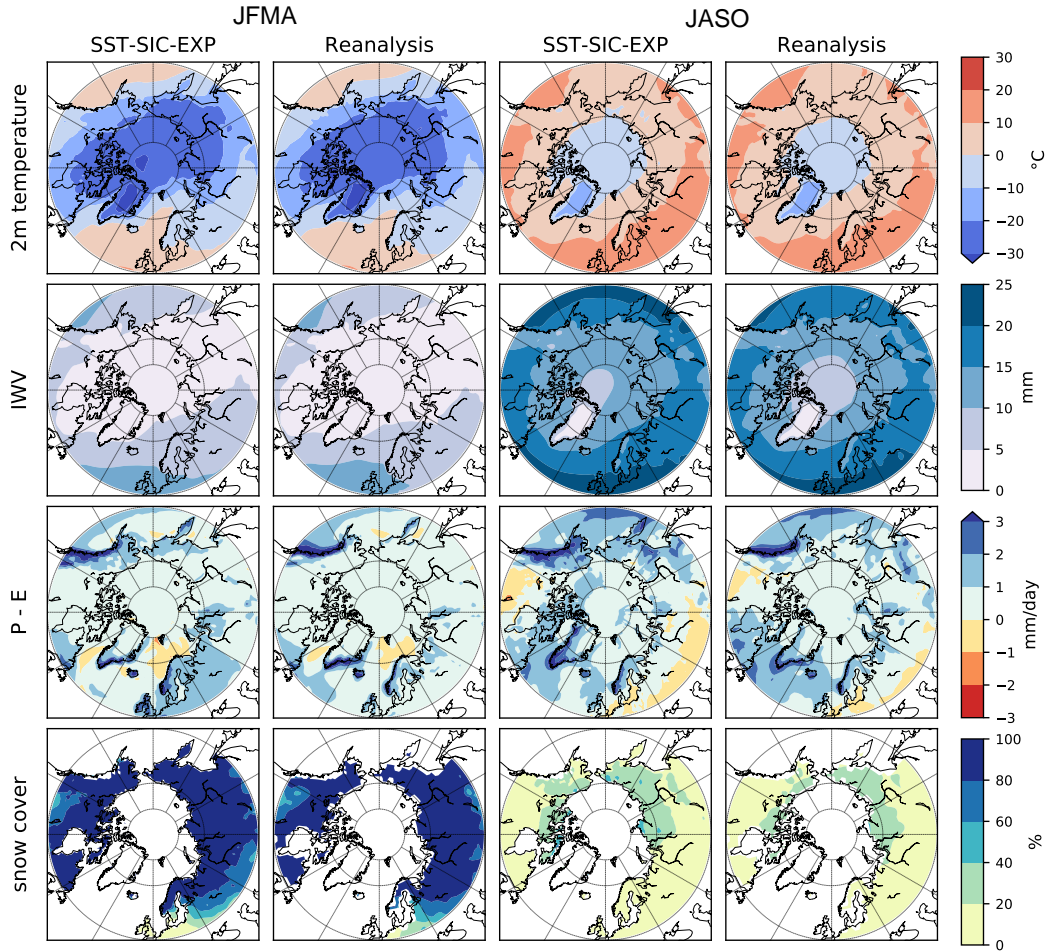


Figure 5: Ensemble mean Arctic seasonal climatology from 1982 to 2014 for the model CAM4 and experiment SST-SIC-EXP compared with the ERA-Interim reanalysis for 2m temperature, IWV and P-E, and NOAA-CIRES for the snow cover.

Generally, the models and experiments reproduce relatively well the spatial climatology. We can see slight local differences but nothing significant, except maybe for net precipitation where higher values can be observed over northern Europe in winter (between 1 to 2 mm) while the reanalysis shows values between 0 and 1 mm. In summer, the values of net precipitation in models are slightly overestimating the reanalysis values for the whole domain. The snow cover has slightly different boundaries; this could come from the lower spatial resolution of the NOAA-CIRES reanalysis.

3.1.2 Annual cycle

We calculated the annual cycle on the ice-free land Arctic domain for all variables. The spatial average was done considering the latitude weighting.

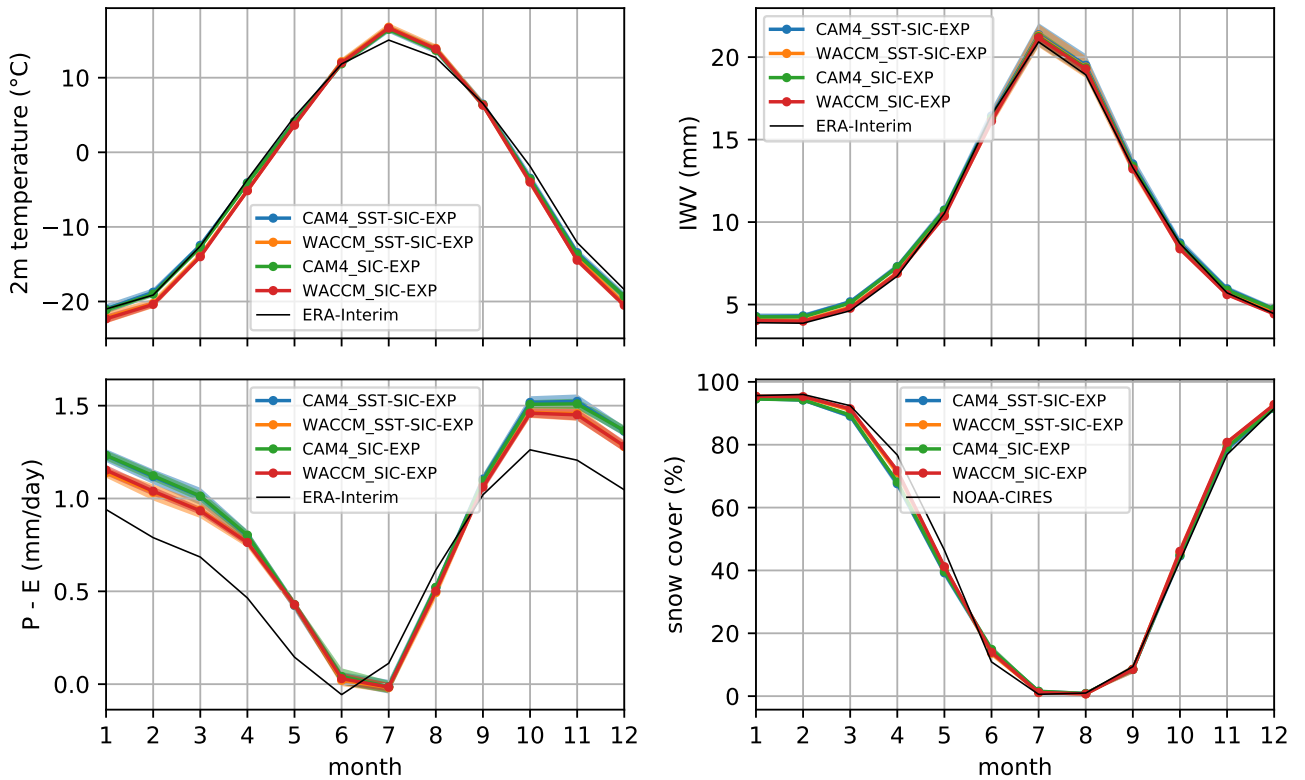


Figure 6: Ensemble mean annual cycle of the climatology from 1982 to 2014 of the ice-free land Arctic domain ($> 50^{\circ}\text{N}$). The light shading around the curves correspond to plus or minus one standard deviation of the interannual variability. The thin black line correspond to the reanalysis.

Figure 6 shows the annual cycle for the four analysed variables. No significant differences have been found between the two experiments. Slightly larger differences were found for the two models: CAM4 and WACCM. CAM4 has slightly higher temperatures (1 to 2°C) and net precipitation (around 0.1 mm/day)

than WACCM around winter. However, the CAM4 snow cover shows slightly lower values (by a few percent) than WACCM around spring. Thus, the slightly higher temperatures seem to lead to more water precipitation or quicker melting. Almost no differences are observed for the IWV.

The black lines on Figure 6 shows values from the reanalyses. The models generally follow relatively well the reanalysis except for net precipitation that is overestimated for almost all months with a temporal shift of the minimum of one month: July instead of June in ERA-Interim. Further analysis (see Appendix B) shows that the precipitation is overestimated around winter whereas in summer both evaporation and precipitation are slightly underestimated, and they compensate each other.

3.1.3 Trends

Unlike the climatology, trends allow seeing the evolution of a variable during a period. Thus, we expect to observe more differences between the two experiments. Trends for SIC-EXP should be due to sea ice variation only, while trends in SST-SIC-EXP are due to both SST and sea ice variations. Figure 7 shows the trends for each variable during the Arctic winter (JFMA) and summer (JASO) for both experiments of the model CAM4 (WACCM is not shown because results are similar). These results need to be taken with caution because the trends simulated by the models are different from the reanalyses trends (see Appendix C).

In the Arctic winter (JFMA), we generally see a smaller number of grid points with significant trends for SIC-EXP than SST-SIC-EXP. However, for the 2m temperature, we see a significant contribution of sea ice variation (SIC-EXP) around the polar cap: a warming around the Barents and Kara seas and south of Greenland (more than $1^{\circ}\text{C}/\text{dec}$), and a cooling north of Canada (less than $-1^{\circ}\text{C}/\text{dec}$). That seems almost only due to sea ice variation (similar patterns for both SST-SIC-EXP and SIC-EXP), whereas the significant warming trends over North Eurasia (around $0.5^{\circ}\text{C}/\text{dec}$) in SST-SIC-EXP disappear in SIC-EXP. Thus, sea ice has a substantial local effect on the 2m temperature but less on the continents. This behavior is similar for the IWV except that we do not observe significant changes in the polar cap. Net precipitation shows less significant trends and the patterns are more irregular. We also observe some significant decrease of snow cover North East Europe (around $-1\%/ \text{dec}$) including a small contribution from sea ice.

For the Arctic summer (JASO) more significant changes are observed for both experiments. The 2m temperature rises significantly all over the Arctic domain with strong warming around the Laptev and Eastern Siberia seas (more than $1^{\circ}\text{C}/\text{dec}$). This time sea ice also has a significant contribution even on lands of about 0 to $0.5^{\circ}\text{C}/\text{dec}$. It is also similar for IWV, but with a substantial rise of water vapor in SST-

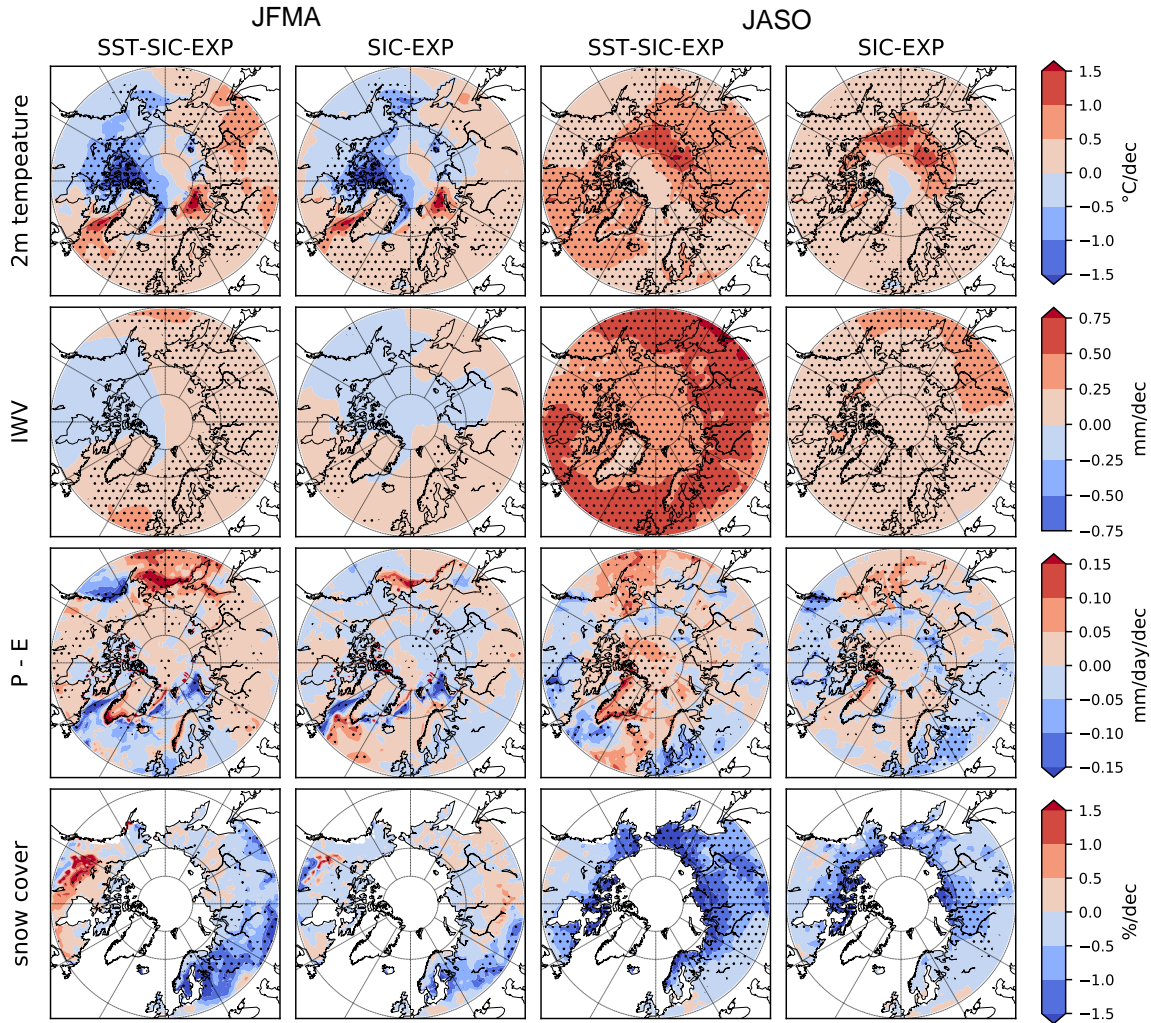


Figure 7: Arctic seasonal trends from 1982 to 2014 of the CAM4 (SST-SIC-EXP and SIC-EXP) ensemble mean. All trends are expressed by decades. The dots represent 95% significance.

SIC-EXP (between 0.25 to 0.50 mm/dec over the ocean and 0.50 to more than 0.75 over lands). Sea ice contributes as well all over the Arctic domain for about 0 to 0.25 mm/dec. About the net precipitation, the trends are still more sparse, however we see slight significant increase around Greenland and north of it with a little contribution from sea ice (less than 0.05 mm/day/dec), while we observe a slight decrease on lands, above all Northern Europe with a more significant contribution of sea ice (around -0.10 mm/day/dec). Snow cover is significantly decreasing above all on top of Siberia (between -1.0 to more than -1.5%/dec) with a slight contribution of sea ice.

3.2 Siberian cooling

This section focuses on the winter (DJF) recent singular WACS pattern shown by *Cohen et al.* (2014) over the period from 1990 to 2013 (Figure 3). We adapted the method of *Ogawa et al.* (2018) to investigate the ability of models and experiments to reproduce the WACS pattern. We use the 2m temperature ERA-Interim as the reference, and we define the Siberian region (70°E - 130°E 40°N - 65°N) to fit the most significant cooling area from this reanalysis. The goal was to evaluate the contribution of sea ice variability for this cooling trend and understand the possible contribution of internal atmospheric variability for this phenomenon by considering each ensemble member separately.

3.2.1 Reanalysis and models comparison

Figure 8 reproduces the conditions of the WACS pattern for the ERA-Interim reanalysis and both models and experiments.

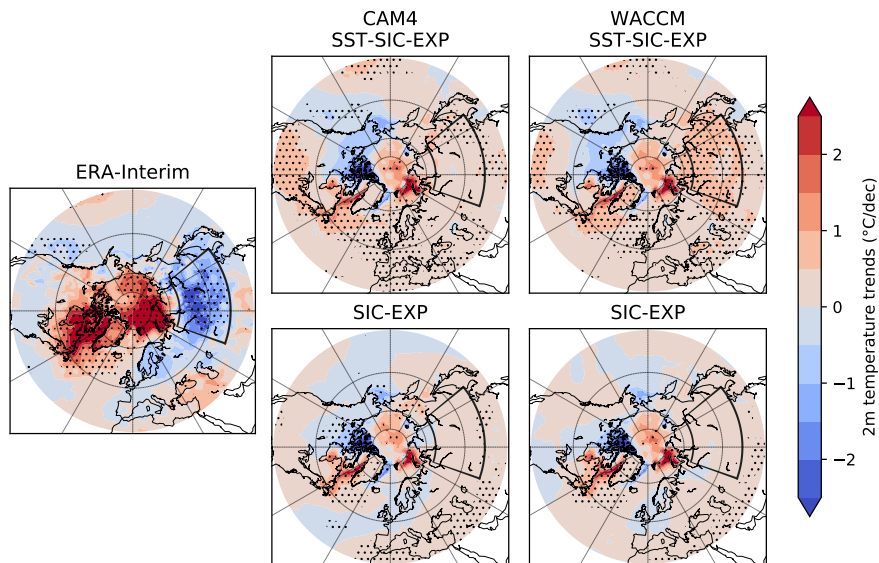


Figure 8: Winter (DJF) trends for the reanalysis ERA-Interim (left) and the ensemble mean of the model CAM4 and WACCM for both experiments from 1990 to 2013 of the 2m temperature. The dots represent 95% significance and the black box represents the Siberian region (70°E - 130°E 40°N - 65°N).

First of all, we see that the reanalysis 2m temperature trends represent relatively well the observations from Figure 3 with a significant cooling over the Siberian region close to $-2^{\circ}\text{C}/\text{dec}$ and two warming centers over the Barents and Kara seas and between North West Canada and Greenland (over $2^{\circ}\text{C}/\text{dec}$). However, the ensemble mean simulations do not reproduce this pattern. We can see slight warming over the two

centers described before, but we also observe a negative trend north of Canada which is not present in the reanalysis. The Siberian cooling is not present for both models and both experiments, and we do not observe any significant trends for this domain, except for WACCM SST-SIC-EXP where a slight significant positive trend is observed (about $1^{\circ}\text{C}/\text{dec}$).

3.2.2 Internal variability

Sea ice changes do not seem to have a significant contribution to the WACS pattern, so maybe it is the consequence of the internal atmospheric variability. A way to investigate this other mechanism is to study each member of the experiments separately. To do that, we computed the spatial average trends over the Siberian region for each member (Figure 9). Only few members show significant trends over this region, and the ones we see are mainly positive except for the member 10 (e10) in CAM4 SIC-EXP that seems to be in the range of the cooling observed in the reanalyses (between -1 to $-2^{\circ}\text{C}/\text{dec}$).

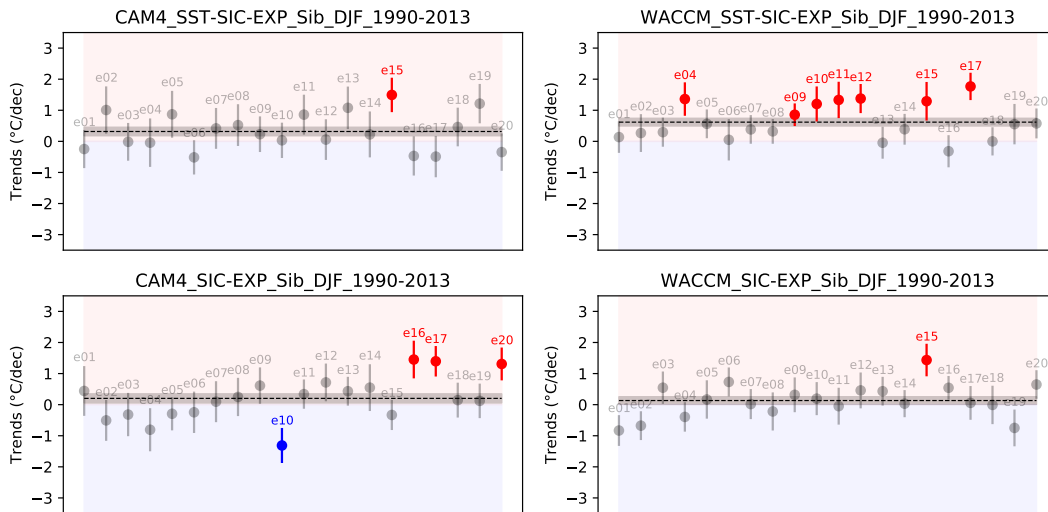


Figure 9: Winter (DJF) 2m temperature trends for each member for both models and experiments from 1990 to 2013 over the Siberian region (70°E - 130°E 40°N - 65°N). The red and blue points correspond to 95% significant trends respectively positive and negative. The vertical bar represent one internannual variability standard deviation ($\pm 1\sigma$) and the dashed line correspond to the ensemble mean trend with $\pm 1\sigma$ shading.

We represent in Figure 10 the member 10 which shows the negative trend in Siberia from Figure 9 beside the ERA-Interim temperature trends. We do observe a similar pattern with a cooling over the Siberian region and a warming around the polar cap. The magnitude is a bit lower as much for the cooling (around $-1.5^{\circ}\text{C}/\text{dec}$ while it goes lower than $-2^{\circ}\text{C}/\text{dec}$ for the reanalysis) than for the warming that goes over

2°C/dec for ERA-Interim while CAM4 SIC-EXP does not exceed so much this limit. It confirms *Ogawa et al.* (2018) results that found only a few members out of a bigger set of models that were able to reproduce the WACS pattern.

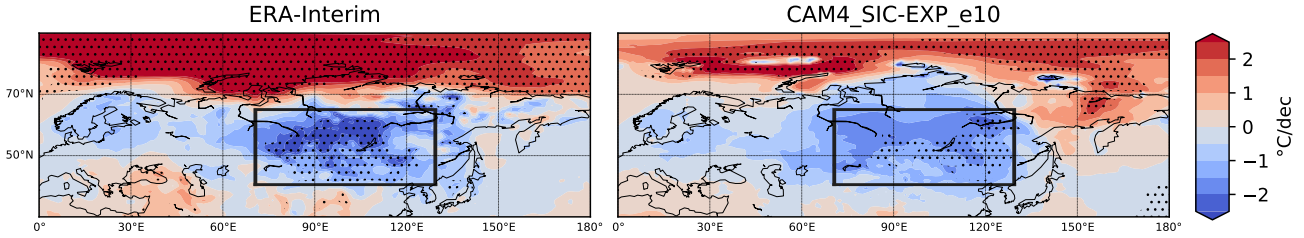


Figure 10: Winter (DJF) 2m temperature trends comparison for ERA-Interim and the member 10 of CAM4 SIC-EXP from 1990 to 2013. The black box represents the Siberian region (70°E-130°E 40°N-65°N) and the dots 95% significance.

3.3 Polar cap moisture budget

The moisture budget is an essential measure of the hydrological cycle. We already discussed the overestimation of net precipitation by models in comparison with ERA-Interim for the annual cycle (Section 3.1.2). Here we compute the net precipitation over the circumpolar Arctic north of 70°N from the two models and ERA-Interim, and we compare it to the moisture flux convergence (right-hand side term from Equation (2)) from ERA-Interim and ECHAM6-FESOM model⁵ which were investigated under the FRAGERUS project (Figure 11).

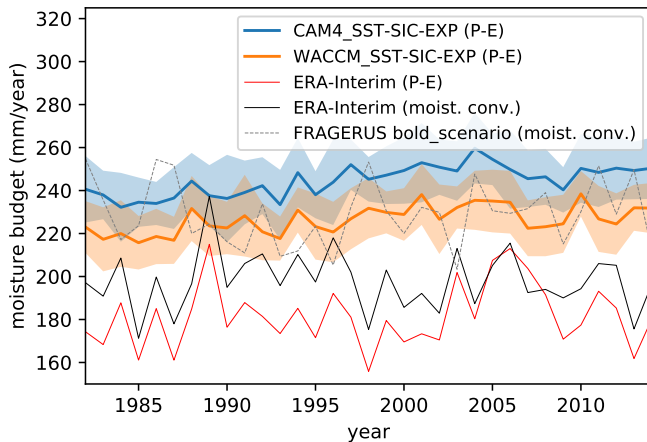


Figure 11: Time series of the annual average moisture budget over the polar cap (>70°N) evaluated with net precipitation and moisture flux convergence (these last data were given by my team from another project FRAGERUS). The CAM4 and WACCM curves correspond to the ensemble mean and the shading correspond to 1σ from all members.

At first, we see that in the reanalysis ERA-Interim net precipitation and moisture fluxes convergence are not equal. *Trenberth et al.* (2011) and *Dufour et al.* (2016) already showed this fact in their study

⁵Atmospheric/Ocean coupled model with spectral resolution T127 and 95 vertical levels.

and noted that the moisture budget of the reanalyses is typically not closed. This difference cannot be explained by the precipitable water tendency (first term of the left-hand side Equation (2)) that varies less than about 1 to 2 mm/year (not shown). Furthermore, we do see a significant difference between models (we show only SST-SIC-EXP because SIC-EXP has a similar range values) and the reanalysis (about 20 to 40 mm/year which generally represents more than 10% of the annual net precipitation). This result is consistent with the light gray curve from the ECHAM6-FESOM model.

4 Discussion

The first results on the Arctic domain generally showed no essential differences between the two models: CAM4 and WACCM. The climatology of the models generally showed a good spatial distribution compared with the reanalyses. The annual cycle exhibits some small differences between models however regarding the reanalyses it is difficult to say if one is better than the other one. The most significant difference we saw is associated with the net precipitation in models and the reanalysis. We did not see large differences between the two experiments in the climatology because the impact of sea ice variation is expected to be seen more in the temporal changes, e.g., trends.

About the impact of sea ice, the trends showed more apparent results. However, the trend values need to be taken with caution because the models do not reproduce well the reanalyses trends. In winter both SST-SIC-EXP and SIC-EXP simulate similar patterns for the 2m temperature. Therefore, the near-surface temperature changes seem associated with the Arctic sea ice changes, except around East Eurasia where the trends look more associated with SST changes. Still, in winter, almost no significant trends can be observed for SIC-EXP for IWV, P-E and snow cover; thus the contribution of sea ice looks less critical. In summer, the magnitude of trends is generally more important, and the distribution for all variables looks more similar between the two experiments with smaller magnitude for SIC-EXP (about one third to half of the SST-SIC-EXP trend values). Therefore, sea ice and SST changes seem to have an impact all over the Arctic domain. This intensification of trends in summer can have a possible link with the minimum sea ice extent (that is generally seen around the end of summer). Sea ice decline leads to more open water, and with an increase of temperature, the moisture exchanges between the ocean and the atmosphere can intensify.

Recent observations (e.g., *Cohen et al. (2014)*, *Wegmann et al. (2018)*) showed the WACS pattern and many studies focused on the possible mechanisms triggering this pattern. Our results confirm the *Ogawa et al. (2018)* conclusion that sea ice by itself does not explain the Siberian cooling. Further study on

members showed that only one member reproduces the WACS pattern in SIC-EXP suggesting that the observed changes are likely associated with internal atmospheric variability. However, this result needs to be taken with caution, because as we saw, the general Arctic warming is not well reproduced by the models (Figure 8). A multimodel study would be needed to reduce the biases of each model and have a better overview of this phenomenon. Furthermore, *He et al.* (2017) showed a strong correlation of the Siberian cooling with the Arctic Oscillation and North Atlantic Oscillation that are large scale modes of climate variability. However, *Wegmann et al.* (2018) showed that the WACS pattern can be linked with the September sea ice in the Barents-Kara Seas.

The last interesting point of this study was the highlight of the excess of moisture convergence over the Arctic. At first, the annual cycle in models showed a significant difference from reanalysis for the net precipitation, and this result was supported by the polar cap moisture budget from the CAM4 and WACCM models but also from the ECHAM6-FESOM model. This point is something that would need further investigation to understand and estimate the possible impact of this gap between models and observations on the Arctic hydrological cycle, especially since *Cohen* (2016) pointed out that many of the current generations of Atmospheric General Circulation Models may lack the ability to simulate the influence of Arctic amplification on mid-latitude climate.

5 Conclusion

We studied two atmospheric models CAM4 and WACCM (that is a “high top” version of CAM4) and two output experiments from *Ogawa et al.* (2018) for the period 1982-2014. These two experiments were designed to show the impact of sea ice independently from the SSTs, and 20 ensemble members were computed to consider the internal variability of the atmosphere.

The climatology and annual cycle did not show significant differences between the two models and experiments. Models are in good agreement with the reanalyses except for the net precipitation that is overestimated in both models. The impact of sea ice was mainly seen in the trends (Figure 7). Polar sea ice can mostly explain the changes around the polar cap for the 2m temperature, otherwise, for other variables, the sea ice contribution on trends is quite smaller than SST changes (about one third to half). The trend magnitudes look more important in summer and can be explained by a possible intensification of the hydrological cycle in conjunction with sea ice decline.

Models are not reproducing the WACS pattern, and sea ice does not appear to have a significant impact for the Siberian cooling. The study of each member showed that the WACS pattern is more likely triggered

by internal atmospheric variability as supported by *Ogawa et al.* (2018). Otherwise, other studies (e.g., *Wegmann et al.* (2018)) found some link between sea ice and the Siberian temperature evolution but the exact phenomenon triggering this pattern is still under debate.

The last result showed an overestimation of the moisture budget over the polar cap in the two models compared to the reanalysis, and it seems to be the case for other models too. Continuing to investigate the Arctic moisture would be essential. Further study to understand the phenomenon would also be necessary to better answer the question asked in this study including more reanalyses and more models.

References

- Bengtsson, L., S. Hagemann, and K. I. Hodges (2004), Can climate trends be calculated from reanalysis data?, *Journal of Geophysical Research*, 109(D11), <https://doi.org/10.1029/2004JD004536>.
- Brutel-Vuilmet, C., M. Ménégoz, and G. Krinner (2013), An analysis of present and future seasonal Northern Hemisphere land snow cover simulated by CMIP5 coupled climate models, *The Cryosphere*, 7(1), 67–80, <https://doi.org/10.5194/tc-7-67-2013>.
- Cohen, J. (2016), An observational analysis: Tropical relative to Arctic influence on midlatitude weather in the era of Arctic amplification, *Geophysical Research Letters*, 43(10), 5287–5294, <https://doi.org/10.1002/2016GL069102>.
- Cohen, J., J. A. Screen, J. C. Furtado, M. Barlow, D. Whittleston, D. Coumou, J. Francis, K. Dethloff, D. Entekhabi, J. Overland, and J. Jones (2014), Recent Arctic amplification and extreme mid-latitude weather, *Nature Geoscience*, 7, 627–637, <https://doi.org/10.1038/ngeo2234>.
- Dee, D. P., and Coauthors (2011), The ERA-Interim reanalysis: configuration and performance of the data assimilation system, *Quarterly Journal of the Royal Meteorological Society*, 137(656), 553–597, <https://doi.org/10.1002/qj.828>.
- Dufour, A. (2016), Transport de vapeur d’eau vers les hautes latitudes : mécanismes et variabilité d’après réanalyses et radiosondages, Ph.D. thesis, thèse de doctorat dirigée par Olga Zolina en Sciences de la Terre et de l’Environnement, Université de Grenoble.
- Dufour, A., O. Zolina, and S. K. Gulev (2016), Atmospheric Moisture Transport to the Arctic: Assessment of Reanalyses and Analysis of Transport Components, *Journal of Climate*, 29(14), 5061–5081, <https://doi.org/10.1175/JCLI-D-15-0559.1>.

- He, S., Y. Gao, F. Li, H. Wang, and Y. He (2017), Impact of Arctic Oscillation on the East Asian climate: A review, *Earth-Science Reviews*, *164*, 48 – 62, <https://doi.org/10.1016/j.earscirev.2016.10.014>.
- Marsh, D. R., M. J. Mills, D. E. Kinnison, J.-F. Lamarque, N. Calvo, and L. M. Polvani (2013), Climate Change from 1850 to 2005 simulated in CESM1(WACCM), *Journal of Climate*, *26*(19), 7372–7391, <https://doi.org/10.1175/JCLI-D-12-00558.1>.
- Neale, R. B., J. Richter, S. Park, P. H. Lauritzen, S. J. Vavrus, P. J. Rasch, and M. Zhang (2013), The Mean Climate of the Community Atmosphere Model (CAM4) in Forced SST and Fully Coupled Experiments, *Journal of Climate*, *26*(14), 5150–5168, <https://doi.org/10.1175/JCLI-D-12-00236.1>.
- Ogawa, F., N. Keenlyside, Y. Gao, T. Koenigk, S. Yang, L. Suo, and al. (2018), Evaluating impacts of recent Arctic sea ice loss on the northern hemisphere winter climate change, *Geophysical Research Letters*, *45*(7), 3255–3263, <https://doi.org/10.1002/2017GL076502>.
- Peixoto, J., A. Oort, E. Lorenz, and A. I. of Physics (1992), *Physics of Climate*, American Inst. of Physics.
- Rogers, R. R., and M. K. Yau (1989), *A short course in cloud physics*, 3rd ed., Pergamon Press Oxford ; New York, ISBN 0-7506-3215-1.
- Serreze, M. C., and R. G. Barry (2011), Processes and impacts of Arctic amplification: A research synthesis, *Global and Planetary Change*, *77*(1), 85 – 96, <https://doi.org/10.1016/j.gloplacha.2011.03.004>.
- Stroeve, J. C., M. C. Serreze, M. M. Holland, J. E. Kay, J. Malanik, and A. P. Barrett (2012), The Arctic’s rapidly shrinking sea ice cover: a research synthesis, *Climatic Change*, *110*(3), 1005–1027, <https://doi.org/10.1007/s10584-011-0101-1>.
- Tilinina, N., S. K. Gulev, and D. H. Bromwich (2014), New view of Arctic cyclone activity from the Arctic system reanalysis, *Geophysical Research Letters*, *41*(5), 1766–1772, <https://doi.org/10.1002/2013GL058924>.
- Trenberth, K. E., J. T. Fasullo, and J. Mackaro (2011), Atmospheric Moisture Transports from Ocean to Land and Global Energy Flows in Reanalyses, *Journal of Climate*, *24*(18), 4907–4924, <https://doi.org/10.1175/2011JCLI4171.1>.
- Wegmann, M., Y. Orsolini, and O. Zolina (2018), Warm Arctic-cold Siberia: comparing the recent and the early 20th-century Arctic warmings, *Environmental Research Letters*, *13*(2), 025,009, <https://doi.org/10.1088/1748-9326/aaa0b7>.

A IWV uncertainty estimation

Figure 12 shows the defined values of specific humidity q for the first 2 pressure levels (1000 hPa and 925 hPa) and the surface pressure upper to these levels. The first column shows that we are missing values of q for the level 1000 hPa where the surface pressure is going upper than 1000 hPa, above all in the NH north of 50°N . This forces us to interpolate the surface value of q to the next level so 925 hPa for this example. As we can see, the maps fit better for the level pressure 925 hPa and this follows on the next levels (this is similar for all models, experiments and time), so the problem is above all for the first level pressure close to the Arctic region. It is probably a problem of time resolution: when the monthly mean is performed it is possible that few days, the moisture value at the level 1000 hPa is not defined and then the monthly mean value at this level is not able to be computed even if the mean pressure level is upper to 1000 hPa.

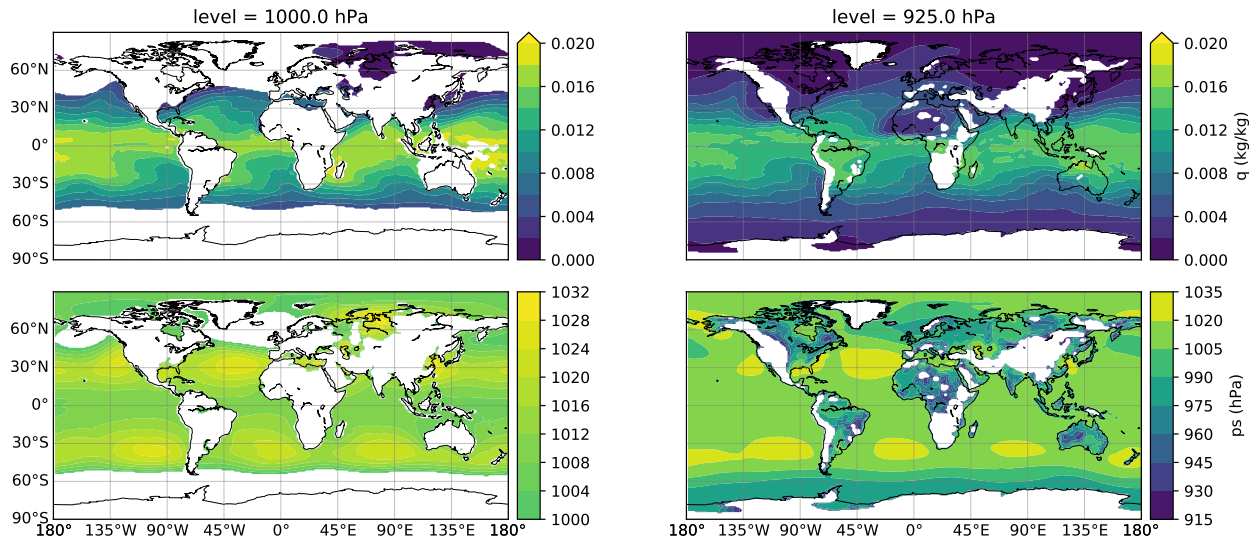


Figure 12: Example of data from the first experiment, model CAM4, first member (e01) for the monthly mean values of January 1982. On top is the specific humidity for the first pressure level at 1000 hPa (left) and the second pressure level at 925 hPa (right). On the bottom, are the surface pressures that exceed the corresponding specific humidity level pressure.

To evaluate a likely magnitude error, let us take a value in the Arctic that is available at 1000 hPa, like for example around 60°N and 80°E . It is interesting because there is an inversion of q as shown in figure 13.

As we can see the vertically integrated value of q is different if we interpolate from 1000 hPa or 925 hPa. In this case, we would overestimate the integral by about 5.4%. Knowing that in some places we can have

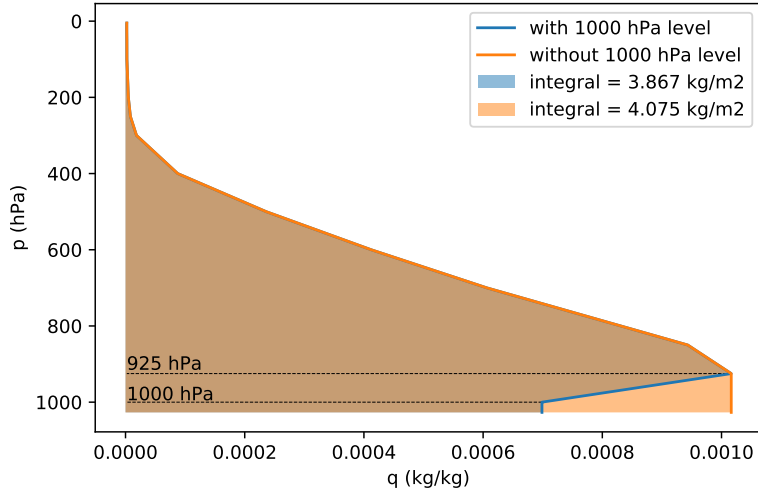


Figure 13: Same data as figure 12 with the specific humidity profile at 59.84°N and 80°N with in blue the interpolated value from the first pressure level 1000 hPa to the surface and in orange the same from the second level 925 hPa.

an inversion or not, that spatial data of the IWV needs to be taken with caution. It may be better after spatial averaging if non-inversion profiles compensate inversions, but we would need to investigate a little more some data to conclude on this.

B Net precipitation

We have seen an overestimation of net precipitation by models in the annual cycle (Figure 6). The question asked in this appendix is to know first if there is a problem in the computation of net precipitation and if not, from which term does it come: precipitation or evaporation?

To check the first possibility (error of computation), we applied the same method of computation for the evaporation that we applied for models but with the ERA-Interim reanalyses latent heat flux and skin temperature (Section 2.3.3). We kept the sea ice and snow cover from the models for simplification. The result is shown on the Figure 14 and even if we applied a little simplification, the results are almost exactly the same. This validates our computation method.

Now we want to know if the differences between models and reanalysis are coming more from the precipitation or the evaporation. Figure 15 decomposes the net precipitation between the precipitation and the evaporation.

As we can see the error is mainly due to an overestimation of the precipitation from September to May

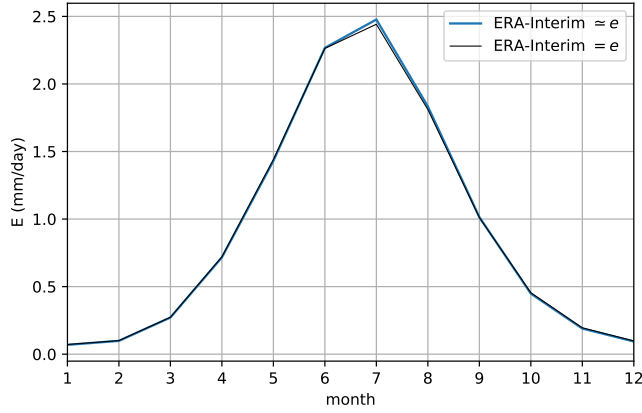


Figure 14: Ice-free land Arctic annual cycle from the period 1982-2014 of the ERA-Interim evaporation (black curve) and from the computation method of Section 2.3.3 with ERA-Interim latent heat flux and skin temperature (blue curve).

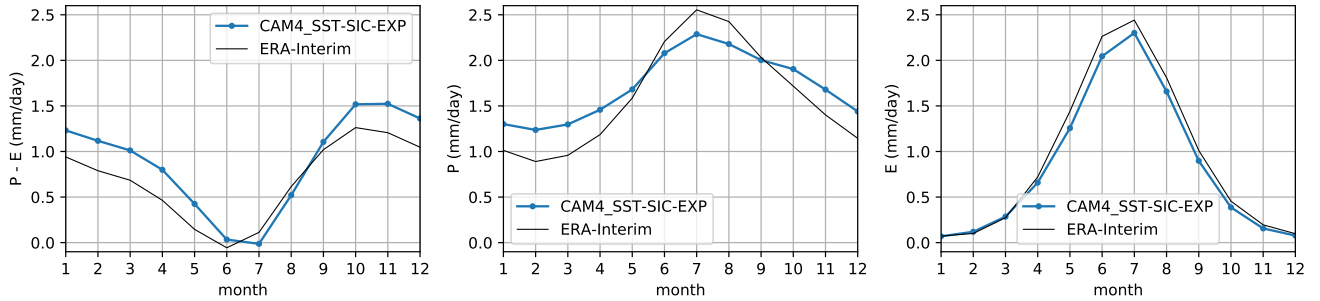


Figure 15: Ice-free land Arctic annual cycle from the period 1982-2014 of net precipitation (left), precipitation (center) and evaporation (right). The black curve corresponds to the ERA-Interim reanalysis and the blue curve is the ensemble mean from CAM4 SST-SIC-EXP.

by the models compared to the ERA-Interim reanalysis while no significant differences can be seen for the evaporation. From May to September the precipitation and evaporation are this time underestimated and balance each other more or less, this is consistent with that fact that net precipitation does not show big differences around this period.

C Reanalyses and model comparison for trends

Figure 16 shows the seasonal reanalysis trends compared to the most realistic experiment SST-SIC-EXP for the model CAM4 (similar result for WACCM) during the period 1982-2014 for the four studied variables. We can see that the differences are generally notable. Especially for the 2m temperature in winter where the

model does not reproduce the strong warming above the polar cap in ERA-Interim (more than $1^{\circ}\text{C}/\text{dec}$) and opposite it shows a strong cooling (less than $1^{\circ}\text{C}/\text{dec}$) north of Canada. These differences are smaller in summer for the 2m temperature while it is the opposite for the IWV: different spatial distribution in winter but with similar ranges and a different pattern for the summer between the reanalysis and the model. It is similar for net precipitation and snow cover.

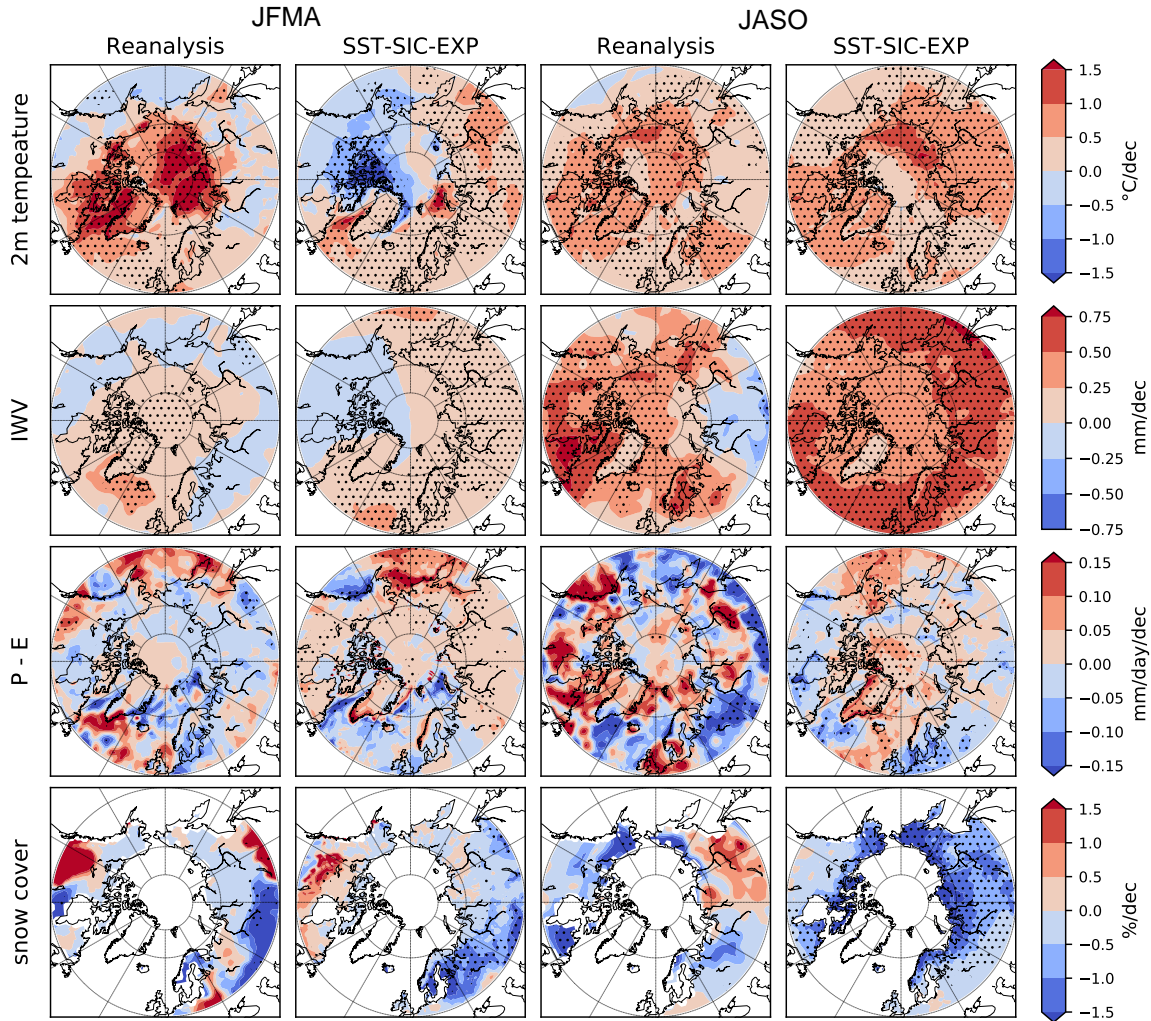


Figure 16: Reanalysis and ensemble mean of the model CAM4 (SST-SIC-EXP) Arctic seasonal trends from 1982 to 2014. All trends are expressed by decades. The dots represent 95% significance. The reanalysis ERA-Interim was used for the 2m temperature, IWV and net precipitation, and NOAA-CIRES for the snow cover.

These differences cannot be explained by the uncertainties of the linear regressions (Figure 17). Indeed, the errors generally do not exceed 10% of the values from Figure 16, except for the snow cover where we can see errors near from 100% in specific areas.

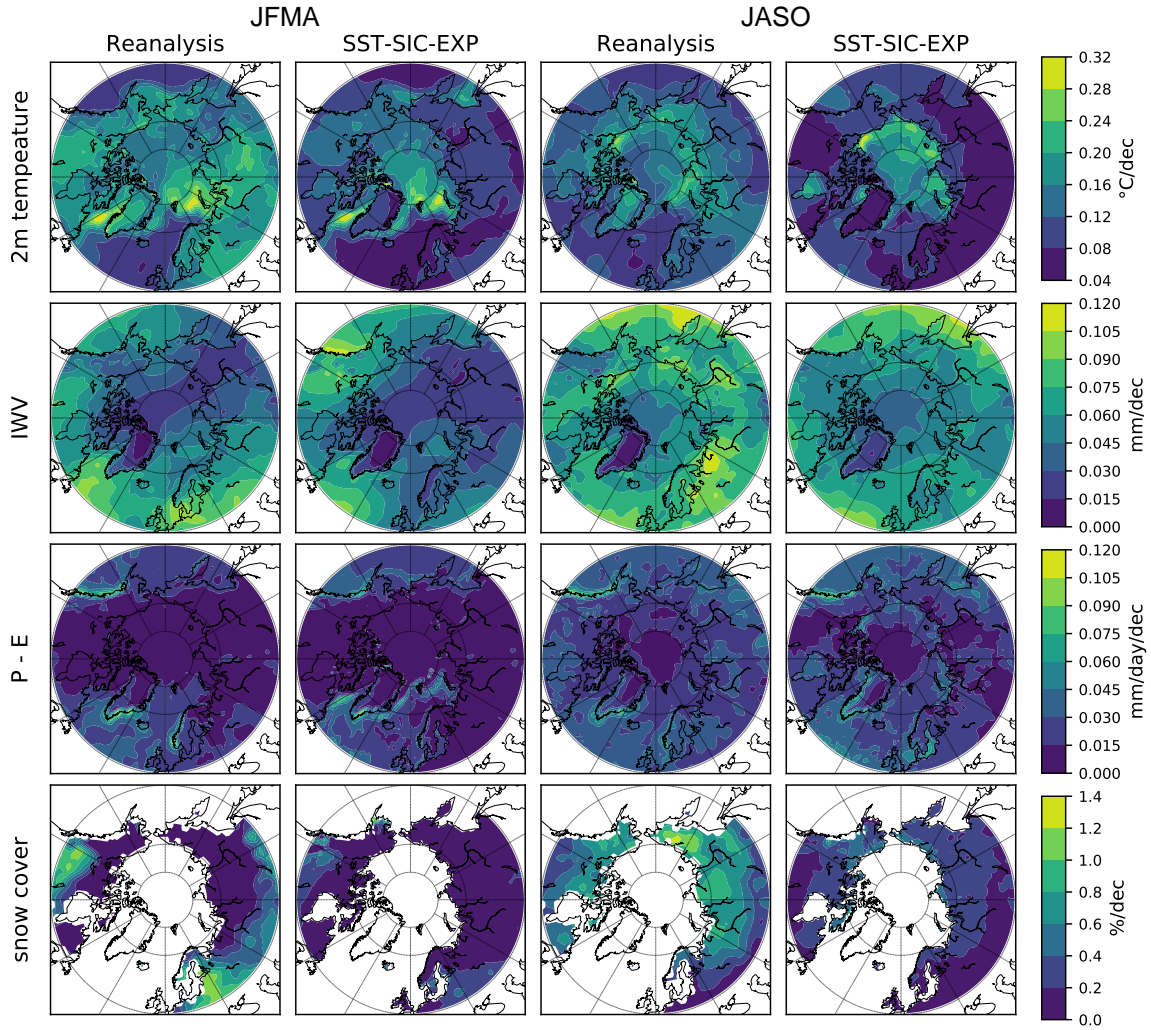


Figure 17: Reanalysis and ensemble mean of the model CAM4 (SST-SIC-EXP) Arctic seasonal standard deviation of the linear regression from 1982 to 2014. The reanalysis ERA-Interim was used for the 2m temperature, IWV and net precipitation, and NOAA-CIRES for the snow cover.

Either, the reanalysis trends are dominated by internal atmospheric variability over this time period so that the ensemble mean is not able to reproduce these trends. Either, the models CAM4 and WACCM do not reproduce well the time evolution of the studied variable over the Arctic domain. A further study on more models, reanalyses and time periods would be needed to answer these last questions.